

## Multi-keV Electron Generation in the Interaction of Intense Laser Pulses with Xe Clusters

Y. L. Shao, T. Ditmire, J. W. G. Tisch, E. Springate, J. P. Marangos, and M. H. R. Hutchinson

*Blackett Laboratory, Prince Consort Road, Imperial College of Science, Technology, and Medicine,  
London, SW7 2BZ, United Kingdom*

(Received 20 March 1996)

We have observed the production of multi-keV electrons through the irradiation of Xe clusters by an intense, near infrared, femtosecond laser pulse. We find the electron kinetic energy distribution consists of two features, a “warm” peak of between 0.1 and 1 keV and a “hot” peak of energy between 2 and 3 keV. These measurements are consistent with a picture of rapid electron collisional heating in the cluster and exhibit good agreement with numerical modeling of the electron energy distribution. [S0031-9007(96)01420-2]

PACS numbers: 36.40.Vz, 33.80.Rv, 36.40.Gk

Though the nature of intense, short pulse laser interactions with single atoms and solid targets has been the subject of extensive experimental and theoretical investigation over the last 15 years [1], the dynamics of intense laser interactions with large molecules and atomic clusters has scarcely been studied during this time. The production of highly charged ions from individual atoms through multiphoton [2] and tunnel ionization [3] in a strong field has been thoroughly researched, as have the energy distributions of the electrons produced during these interactions [above threshold ionization (ATI)] [4–6]. Concurrently, the production of hot, high density plasmas by the intense irradiation of a solid by a short pulse laser has also been the subject of detailed studies [7,8]. Experiments on individual atoms have confirmed that the majority of electrons released by single atoms in a laser field of intensity  $<10^{16}$  W/cm<sup>2</sup> typically exhibits kinetic energies of  $<100$  eV [6]. Interactions with solids, on the other hand, have been shown to be much more efficient at coupling laser energy into electron energy. The electron temperature in these experiments is, however, usually clamped at a few hundred eV due to the conduction of the laser energy into surrounding cold, bulk material [9].

Only recently has the nature of intense laser interactions with van der Waals bonded atomic clusters of 20–100 Å been addressed in experiments. These experiments have suggested that the laser-cluster interaction is much more energetic than that of isolated atoms, producing bright x-ray emission (100–5000 eV photons) when a low density gas containing clusters is illuminated [10–12]. The interactions also appear to be quite different than those of laser solid target interactions since a cluster, though like a solid, having high local density and therefore a high collision frequency, is unlike a solid because it is an isolated system, much smaller than a laser wavelength. Consequently, the laser interacts uniformly with all the atoms, much more like the interaction of a laser with a low density gas. Recent experiments by Ditmire *et al.* have indicated that the electrons in a cluster undergo rapid collisional heating for the short time ( $<1$  ps) before the cluster disassembles in the laser [11]. These measurements indicated indirect evi-

dence for keV electron production in the cluster through time resolved x-ray spectroscopic data. In fact, irradiation of Xe clusters at intensities near  $10^{19}$  W/cm<sup>2</sup> with 248 nm light has shown some evidence of multi-keV electron production through the observation of x rays with energies up to 5 keV [10]. Evidence for high energy ion production in Ar clusters has also been observed [13]. In contrast to the extensive knowledge of electron energy distributions from atoms, however, no direct data on the exact nature of the electron kinetic energies produced by the intense irradiation of clusters exist. In this Letter we present the first energy distribution measurements of electrons produced during the interaction of a femtosecond laser pulse with Xe clusters.

Our experiment used a chirped pulse amplification Ti:sapphire laser, described previously [14]. This system is capable of delivering 40 mJ, 150 fs pulses at a wavelength of 780 nm. The linearly polarized laser pulse was focused with an  $f/30$  lens into a time-of-flight (TOF) chamber, yielding a peak intensity of about  $1 \times 10^{16}$  W/cm<sup>2</sup>. The absolute peak intensity of the laser has been confirmed by observing the appearance of He<sup>2+</sup> via tunnel ionization (which occurs at an intensity of  $\sim 7 \times 10^{15}$  W/cm<sup>2</sup>). The time-of-flight chamber was evacuated to a base pressure of  $10^{-7}$  mbar. The acceptance angle of electrons produced at the focus was limited to an angle of 5° from the interaction region by a small aperture. Two closely spaced grids were placed behind the entrance aperture to the TOF drift tube. The first grid was connected to a voltage supply to stop electrons below a selected energy; the second was grounded to ensure that the drift region was field free. A two stage microchannel plate was used to detect the electrons.

The Xe clusters were produced with a solenoid valve pulsed sonic gas jet with a nozzle aperture of 0.6 mm. With sufficiently high backing pressure, clusters form in the gas jet flow due to the cooling associated with the adiabatic expansion of the gas into vacuum [15]. The jet was operated with a backing pressure range from 0 to 5 bar. A skimmer with a 0.5 mm aperture and 50° cone located 20 cm below the gas jet was used to separate the main

chamber from a secondary chamber and served to produce a low density cluster beam which intercepted the laser beam at the laser focus. The electron signal was observed only when the laser pulse and the arrival of the clusters from the gas jet were coincident. The presence of Xe clusters in the flow from our gas jet has been confirmed through a series of Rayleigh scattering measurements in the gas jet [see below, Fig. 2(a)]. These measurements indicated that the clusters formed reach an average diameter of  $50 \pm 5 \text{ \AA}$  with a jet backing pressure of 4.5 bars. Previously determined scaling laws for clustering in Xe indicate that clusters from our jet are composed of 1000–2000 atoms per cluster [16], corresponding to a cluster diameter of 50 to 60  $\text{\AA}$ , respectively, in good agreement with our measurement. These scaling laws also suggest that essentially all of the Xe atoms coming from the jet have condensed into clusters [16].

The energy spectrum of the electrons produced during the irradiation of these 50 $\text{\AA}$  clusters (4.5 bars backing pressure) with an intensity of  $1 \times 10^{16} \text{ W/cm}^2$  is shown in Fig. 1(a). This spectrum was found by measuring the elec-

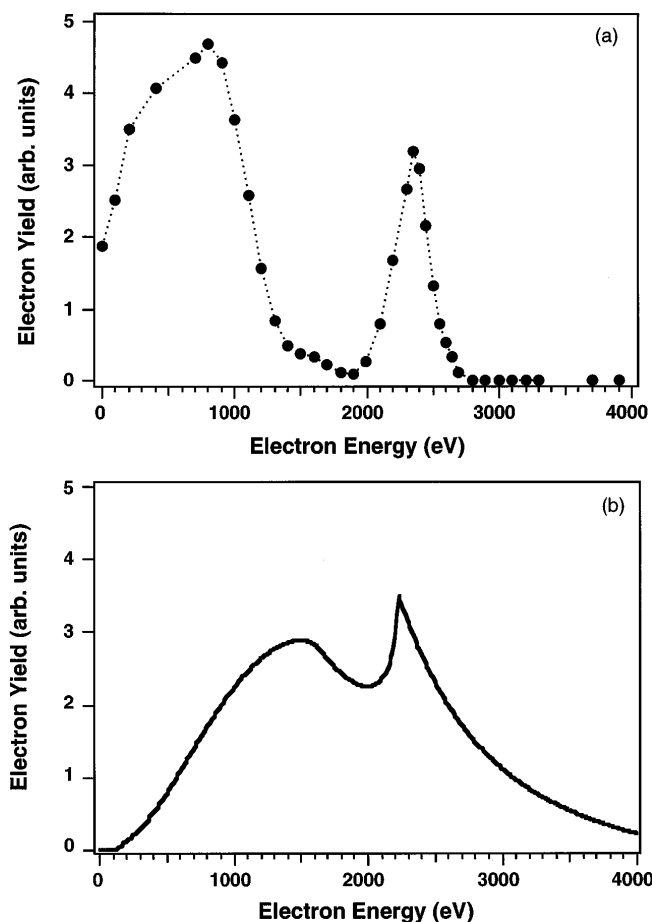


FIG. 1. (a) Measured electron kinetic energy distribution from Xe clusters for a peak intensity of  $1 \times 10^{16} \text{ W/cm}^2$ . The gas jet backing pressure was 4.5 bars (corresponding to an average cluster size of 50  $\text{\AA}$ ). (b) Calculated electron energy distribution for a peak intensity of  $1 \times 10^{16} \text{ W/cm}^2$  and a cluster size of 50  $\text{\AA}$ .

tron yield in the direction of the laser polarization as a function of retarding voltage and then differentiating the result. Each point represents the average of 50 laser shots in a laser energy bin of  $\pm 10\%$ . The most remarkable aspect of this energy distribution is the presence of a large fraction of the electrons with between 2 and 3 keV of kinetic energy. Previous measurements of ATI spectra from single atoms at this intensity and pulse duration have indicated that the vast majority of the electrons produced exhibit energy below 100 eV [4,6]. Only a very small fraction of electrons (typically  $10^{-3}$  or  $10^{-4}$  of those produced) have higher energy, with no detectable electrons having energy above 1 keV [6]. The spectrum observed from the Xe clusters clearly exhibits a much greater coupling of laser energy to hot electrons than is present during the irradiation of single atoms. Furthermore, this spectrum indicates that the laser cluster interaction produces hotter electron temperatures than during traditional solid target illumination at this intensity, where electron temperatures of 100 to 500 eV are usual [9].

Another striking aspect of the shape of the electron energy spectrum is the presence of two distinct features in the distribution. The first, broad lobe consists of what we shall refer to as “warm electrons” with energy ranging from 0.1 out to 1 keV. A second, more sharply defined peak appears at 2.5 keV, referred to as the “hot electrons.” Though the two peaks seem distinct, we emphasize that both are present only when the laser interacts with Xe clusters. We have also attempted to characterize electron energies resulting from the interaction of the laser with individual Xe atoms in a backfill of Xe gas in the TOF chamber. For this measurement we filled the chamber with a Xe pressure of  $10^{-7}$  torr, a pressure at which space charge effects are negligible. We detected no electrons with energy above 100 eV.

That this signal is the result of the laser-cluster interaction can also be seen by examining the dependence of the hot electron yield as a function of gas jet backing pressure. Figure 2 illustrates the close correlation of the onset of hot electron production with the onset of clustering as determined by Rayleigh scattering in the gas jet [11]. The onset of cluster production was observed by monitoring the  $90^\circ$  Rayleigh scattered signal from a 10 ns, 532 nm laser pulse traversing the gas jet. The scattered signal is illustrated in Fig. 2(a). This curve indicates that clusters of significant size ( $\geq 20 \text{ \AA}$ ) begin to be formed in our jet with a backing pressure of  $>1$  bar. Production of hot electrons, measured by integrating the TOF signal over an appropriate temporal gate, as a function of backing pressure is shown in Fig. 2(b). The onset of hot electron production with a 1 bar backing pressure is quite closely correlated to the observed onset of clustering in Fig. 2(a). The warm electron production above 100 eV is also closely correlated with the onset of clustering at 1 bar backing pressure.

The presence of two distinct peaks in the energy distribution suggests that these two lobes may be produced

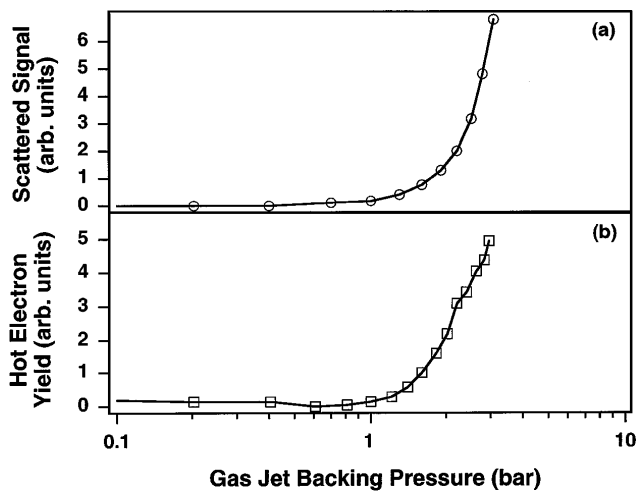


FIG. 2. (a) Measured Rayleigh scattered signal as a function of Xe backing pressure. (b) Measured yield of hot electrons for a peak intensity of  $1 \times 10^{16} \text{ W/cm}^2$  as a function of Xe backing pressure.

under different conditions within the cluster, at different times during the laser pulse. This supposition seems to be supported by the angular distribution of the emitted electrons with respect to the laser polarization. The angular distribution of the electrons was found by rotating the polarization of the laser pulse with respect to the acceptance direction of the detector with a  $\lambda/2$  plate placed before the focusing lens. A  $-300 \text{ V}$  potential was placed on the grids to repel any low energy electrons that may be produced by impurities. The distribution of the warm electrons was differentiated from that of the hot electrons by exploiting the different flight times of the two lobes in the distribution and time gating the signal. The measured distribution of the warm electrons is shown in Fig. 3(a) and that of the hot electrons is shown in Fig. 3(b).

The warm electrons exhibit a broad angular distribution, peaked around the laser polarization axis. The distribution of warm electrons shows a peak at  $0^\circ$  (along the laser polarization) with a width of about  $60^\circ$  (full width at half maximum). This distribution displays significant differences from earlier reported work on atoms. The electrons associated with high order tunneling ATI are expected to have an angular distribution with a narrow peak at  $0^\circ$ . (A width of  $15^\circ$ – $20^\circ$  was reported in Ref. [4].) In high field tunneling ionization, the narrow peak in electron release stems from the high tunneling rate in the direction of the laser electric field. The warm electrons observed in our experiment, therefore, cannot be interpreted as originating simply from tunnel ionized electrons from individual atoms. Some rescattering of the electrons by charged ions in the cluster is necessary to explain the broad distribution observed. Even more dramatic is the angular distribution of the hot electrons [Fig. 3(b)]. The emission of the hot electrons is isotropic with no significant variation with respect to the laser polarization.

To further illuminate the physics of the laser-cluster interaction we have conducted numerical modeling of the dy-

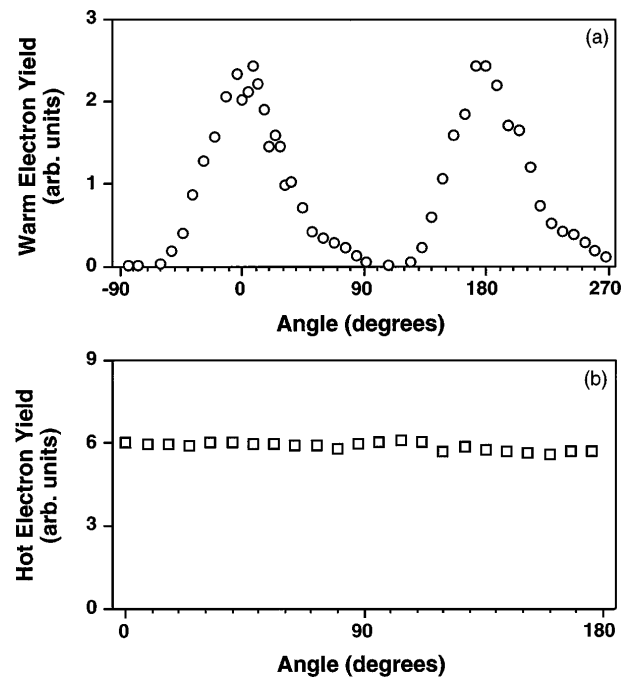


FIG. 3. (a) Angular distribution of electrons in the 0.3 to 1 keV range. Emission along the laser electric field polarization is defined at  $0^\circ$  and  $180^\circ$ . (b) Angular distribution of electrons produced in the 2 to 3 keV range.

namics. The aim of the model is to calculate the extent of electron collisional heating (inverse bremsstrahlung) in the laser field. The details of this model have been described previously [12]. In brief, the model treats the cluster as a spherical microplasma, subject to the standard processes of a laser heated plasma. The model solves for ionization in the cluster, including rates for laser field tunnel ionization and both thermal and laser driven electron collisional ionization. Laser driven collisional heating in the cluster is found using the standard Silin formulas for the electron-ion collision frequency [17]. The model calculates the rate of electrons leaving the cluster by free streaming, accounting for the mean free path of electrons in the cluster. Only electrons with energy sufficient to overcome the Coulomb attraction of the positively charged cluster are allowed to leave. The cluster expansion, assumed to be uniform and isotropic, is calculated accounting for hydrodynamic and Coulomb repulsion forces within the charged cluster. The electron energy distribution within the cluster is assumed to be Maxwellian throughout the calculation.

The electric field inside the cluster is calculated using the formula for the electric field of a dielectric sphere in a uniform electric field (accurate since the cluster is much smaller than the laser wavelength). The electric field in the cluster is therefore

$$E = E_0(3/|\epsilon + 2|), \quad (1)$$

where  $E_0$  is the laser electric field in vacuum. The cluster dielectric constant is given by the Drude model for a plasma:  $\epsilon = 1 - (n_e/n_{\text{crit}})(1 + i\nu/\omega)^{-1}$ , where

$n_e$  is the electron density,  $n_{\text{crit}}$  is the electron critical density for a laser field of frequency  $\omega$ , and  $\nu$  is the electron ion collision frequency. Evidence for the shielding that occurs in Eq. (1) when  $n_e/n_{\text{crit}} > 3$  has previously been observed in the behavior of high order harmonics produced in Ar clusters [18]. Equation (1) has a sharp maximum when  $n_e/n_{\text{crit}} = 3$ . At this point the cluster undergoes rapid collisional heating because of an enhancement of the field in the cluster. This resonance is similar to the giant resonance in light absorption observed in metallic clusters [19].

The calculated electron distribution for a 50 Å Xe cluster subject to a 150 fs Gaussian, 780 nm pulse with a peak intensity of  $10^{16}$  W/cm<sup>2</sup> is shown in Fig. 1(b). The distribution is found by summing the energy distribution of the electrons that leave the expanding cluster during the laser pulse. The calculated distribution exhibits a close similarity to the measured electron distribution, having a two lobed structure. The sharp peak near 2 keV is clearly consistent with the observed data, in both position and its narrow width.

The warm electron portion of the curve in Fig. 1(b) results from electrons that escape from the surface of the cluster early in the pulse, before it has expanded significantly. On the leading edge of the pulse, tunnel ionization creates free electrons in the cluster. Some collisional heating and ionization occurs. Free streaming of warm electrons during this phase accounts for the portion of the electron distribution below 1 keV. The cluster expands predominantly by hydrodynamic forces during the early part of the pulse. Once sufficient expansion has occurred to drop the electron density to  $3n_{\text{crit}}$ , the resonance in Eq. (1) causes rapid heating of the remaining electrons in the cluster. These electrons leave promptly once they have been heated sufficiently to overcome Coulomb forces in the cluster. They account for the sharp peak in the electron distribution at 2 keV.

These calculations seem to explain the prominent features of the observed electron energy distribution. The model calculations indicate that the warm electron peak is the result of collisional heating of electrons near the surface of the cluster on the rising edge of the laser pulse. The hot electrons result from rapid heating of the remaining electrons in the bulk of the cluster later in the pulse when the electron density drops to a point to bring the heating into resonance. This explanation seems to be corroborated by the observed angular distribution data. The warm electrons are the result of some collisional heating early in the pulse. These electrons have undergone a limited number of collisions, broadening the angular distribution from that of purely tunnel ionized electrons. The hot electrons, on the other hand, result from extensive collisional heating of the electrons in the bulk of the cluster. Consequently, their velocity distribution has been completely randomized, accounting for the isotropic distribution observed.

Though the calculated energy distribution exhibits close agreement with the measured distribution in the positions

of the distribution peaks, the calculation does differ from the measured energy spectrum in some features. The calculated distribution in Fig. 1(b), for example, exhibits peaks in the electron distribution that are broader than those observed in the data. This is most likely due to the assumption that the electron distribution within the cluster is a Maxwellian. In reality, the distribution within the cluster will not completely thermalize; the hottest electrons in the outer tail of the distribution leave the cluster first. The fast disassembly of the cluster prevents complete thermalization. This is in evidence in the nonisotropic nature of the warm electron distribution in Fig. 3(a). The model assumes an isotropic electron distribution, which is mirrored in the hot electron distribution. Despite these simplifying assumptions, the numerical calculations of Fig. 1(b) appear to match the observed trends in the kinetic energy data.

In conclusion, we have measured the properties of electrons produced during the interaction of intense, 780 nm, 150 fs laser pulses with Xe clusters. We find that rapid collisional heating of the electrons in the cluster prior to significant expansion yields an electron distribution that exhibits two distinct peaks with energies ranging up to 3 keV. We find that this distribution is reproduced in numerical calculations of the cluster heating. The hot electrons appear to be evidence for a resonance in the electron heating when the cluster electron density drops to three times the critical density. These data indicate that the interaction of an intense laser pulse with small atomic clusters can efficiently couple energy to electrons, exceeding the intense heating of high intensity solid target interactions.

We acknowledge the assistance of M. Mason, N. Hay, and D. Fraser and we thank R.A. Smith for useful conversations. This work was supported by the EPSRC and MOD.

- 
- [1] M. D. Perry and G. Mourou, *Science* **264**, 917 (1994).
  - [2] A. L'Huillier *et al.*, *Phys. Rev. A* **27**, 2503 (1983).
  - [3] S. Augst *et al.*, *J. Opt. Soc. Am. B* **8**, 858 (1991).
  - [4] U. Mohideen *et al.*, *Phys. Rev. Lett.* **71**, 509 (1993).
  - [5] G. G. Paulus *et al.*, *Phys. Rev. Lett.* **72**, 2851 (1994).
  - [6] B. Walker *et al.*, *Phys. Rev. Lett.* **73**, 1227 (1994).
  - [7] M. M. Murnane *et al.*, *Science* **251**, 531 (1991).
  - [8] J. C. Kieffer *et al.*, *Phys. Rev. Lett.* **62**, 760 (1989).
  - [9] R. Shepherd *et al.*, *J. Quant. Spectrosc. Radiat. Transf.* **51**, 357 (1994).
  - [10] A. McPherson *et al.*, *Nature (London)* **370**, 631 (1994).
  - [11] T. Ditmire *et al.*, *Phys. Rev. Lett.* **75**, 3122 (1995).
  - [12] T. Ditmire *et al.*, *Phys. Rev. A* **53**, 3379 (1996).
  - [13] J. Purnell *et al.*, *Chem. Phys. Lett.* **229**, 333 (1994).
  - [14] D. J. Fraser and M. H. R. Hutchinson, *J. Mod. Opt.* (to be published).
  - [15] O. F. Hagena and W. Obert, *J. Chem. Phys.* **56**, 1793 (1972).
  - [16] J. Wormer *et al.*, *Chem. Phys. Lett.* **159**, 321 (1989).
  - [17] V. P. Silin, *Sov. Phys. JETP* **20**, 1510 (1965).
  - [18] T. D. Donnelly *et al.*, *Phys. Rev. Lett.* **76**, 2472 (1996).
  - [19] C. Bréchnignac and J. P. Connerade, *J. Phys. B* **27**, 3795 (1994).